

EPR study of paramagnetic centers in SiO₂:C:Zn nanocomposites obtained by infiltration of fumed silica with luminescent Zn(acac)₂ solution

D.V. Savchenko^{1,2,*}, V.S. Memon¹, A.V. Vasin^{1,3}, D.V. Kysil³, A.V. Rusavsky³, O.P. Kuz¹, F.M. Gareeva¹, E.N. Kalabukhova³

¹National Technical University of Ukraine "Igor Sikorsky Kyiv Polytechnic Institute"
37, prosp. Peremohy, 03056 Kyiv, Ukraine

²Institute of Physics of the CAS,
2, Na Slovance, 18221 Prague, Czech Republic

³V. Lashkaryov Institute of Semiconductor Physics, NAS of Ukraine
41, prosp. Nauky, 03680 Kyiv, Ukraine

*E-mail: dariyasavchenko@gmail.com

Abstract. Silica-carbon with zinc (SiO₂:C:Zn) nanocomposites obtained *via* infiltration with aged luminescent zinc acetylacetonate (Zn(acac)₂) ethanol solution of two concentrations (1 or 4%) into the fumed silica (SiO₂) matrix have been studied using EPR within the temperature range 6...296 K before and after thermal annealing. The EPR spectrum of SiO₂:C:Zn nanocomposites consists of three signals with the Lorentzian lineshape corresponding to paramagnetic centers with $S = 1/2$, which are related to carbon dangling bonds (CDB) ($g = 2.0029(3)$), silicon dangling bonds ($g = 2.0062(3)$) and oxygen-centered carbon-related radicals (CRR) ($g = 2.0042(3)$). A small EPR linewidth (<1 mT) observed for CDB and oxygen-centered CRR allows us to conclude that they are in the sp^3 -hybridized state. It was found that the temperature dependence of the EPR signal integrated intensity of the CDB and oxygen-centered CRR follows the Curie–Weiss law with a small positive value of the Curie–Weiss constant, which indicates that the weak ferromagnetic exchange interaction takes place in the spin system of CDB and oxygen-centered CRR. It was supposed that the carbon-related centers are clustered in SiO₂:C:Zn nanocomposites. We assume that the oxygen-centered CRR in the sp^3 -hybridized state are associated with luminescent centers in previously reported aged Zn(acac)₂/C₂H₅OH solution.

Keywords: silica-carbon nanocomposites, carbon-related centers, dangling bonds, exchange interaction, electron paramagnetic resonance.

<https://doi.org/10.15407/spqeo24.02.124>
PACS 75.75.-c, 76.30.-v, 81.05.uj

Manuscript received 24.03.21; revised version received 29.04.21; accepted for publication 02.06.21; published online 16.06.21.

1. Introduction

Nanostructured composites are known as perspective materials for nanosized devices with multifunctional and high operational characteristics. The development of effective approaches to formation of the nanostructured systems allows realizing principally new technological solutions to the development of materials for nanosized devices, ultra-compact sensors, catalyst carriers, sorbents, and modern energy sources.

In recent decades, the synthesis of inorganic nanocomposites is intensively developed, owing to their

special physicochemical properties and the prospect of developing new effective adsorbents, catalysts, energy sources, sensors, and composite materials on its basis.

The practical application of the nanocomposites based on fumed silica (SiO₂) and transition or rare-earth metal oxides is defined both by their composition and structure, including the particle size of metal-containing phases and their bonding to the silica matrix [1]. The use of the metal-organic salts, especially their hydrates, in the chemical modification of fumed silica allows obtaining the nanocomposites containing nanosized particles of metal oxides distributed over the silica matrix [2].

Chemical modification of the silica surface with metal compounds is one of the synthesis stages of the carbon-oxide nanocomposites $C/M_xO_y/SiO_2$, where M is the metal atom of modifying reagent [3]. During pyrolysis of the organic compounds in the inert atmosphere, the carbon structures are formed both inside the pores and on the outer surface of silica particles. The hybrid carbon-oxide adsorbents have essential differences from the mechanical mixture of individual materials defined by formation conditions and distribution of carbon components in nanocomposites [4, 5]. As a rule, the resulting carbon reveals high density, low volume of micropores, and low specific surface. The carbon, which was obtained by pyrolysis of high-molecular compounds adsorbed on the silica matrix, forms the structures determined by precursor structure and synthesis conditions allowing variation of the structural properties inherent to the resulting materials [3].

The silica-carbon composites with the carbon content of 6.5% and zinc concentration of 10.98% were obtained by impregnation of silica gel by zinc acetylacetonate ($Zn(acac)_2$) in [6]. It turned out that during the $Zn(acac)_2$ pyrolysis, the zinc silicate (Zn_2SiO_4) along with carbon precipitate is formed. The zinc silicate is formed on the silica gel surface, and carbon precipitate is non-uniformly distributed over the surface.

As was found in [7], during the high-temperature pyrolysis of $Zn(acac)_2$ into the silica gel pores, the hydrophilic properties of the surface suddenly disappear. At the same time, the heterogeneous carbon layer is located on the adsorbent surface, where the carbonized fragments mainly consist of individual hydroxyl groups. In the case of carbonization of $Zn(acac)_2$ into the silica gel pores, the hydration properties of the obtained silica-carbon nanocomposites and initial silica are very similar. This effect was explained by formation of the Zn_2SiO_4 layer on the surface. It was suggested that the carbon component of the surface is mainly localized in the narrowest pores of adsorbent that are unavailable for the $Zn(acac)_2$ molecules because of their geometrical sizes.

Recently, the clustering process of ZnO and formation of nanoparticles in an ethanol solution of $Zn(acac)_2$ by the “natural aging” process at room temperature without specific heating was reported in [8, 9]. The ethanol solutions of $Zn(acac)_2$ of various concentrations (0.4...10%) aged for three months were investigated using the photoluminescence (PL) method. During aging, the initial colorless solution gradually changed its color to yellow. It should be noted that at a high concentration of $Zn(acac)_2$ (10%), this effect was not observed. These changes were accompanied by intense visible broadband PL within the spectral range 375...600 nm. The detailed study of PL emission/excitation showed that the emission band consists of two bands centered at 420...450 nm and 500 nm with corresponding excitation bands at 365 nm and 420 nm. The infrared spectroscopy and PL analysis allowed authors to assume that PL in aged $Zn(acac)_2/C_2H_5OH$ is related to the sub-nanometer Zn:O:C clusters/agglomerates.

In this work, the electron paramagnetic resonance (EPR) technique was applied to study the paramagnetic centers present in $SiO_2:C:Zn$ nanocomposites with the aim to find out the type of defect, which can be responsible for the PL properties previously observed in $SiO_2:C:Zn$ nanocomposites. To this end, we have investigated the EPR spectra in the aged luminescent $Zn(acac)_2$ solution of various concentrations, which was infiltrated into the fumed silica matrix.

2. Materials and methods

The initial fumed silica with a specific surface close to $295\text{ m}^2/\text{g}$ and average particle size of 10...12 nm was obtained from the State Enterprise “Kalush Test Experimental Plant of Institute of Surface Chemistry, National Academy of Sciences of Ukraine”. The silica-carbon nanocomposites with zinc ($SiO_2:C:Zn$) were obtained using infiltration of aged luminescent zinc acetylacetonate ($Zn(acac)_2$) ethanol solution of two concentrations (1 and 4%) into the fumed silica matrix. As a result, the silica-carbon $SiO_2:C:Zn$ samples with Zn_2SiO_4 on their surface were prepared. The thermal annealing of the samples was carried out at $600\text{ }^\circ\text{C}$ in air.

The EPR measurements were performed using the Bruker ELEXSYS EPR E580 spectrometer with ER 4122 SHQE SuperX High-Q cavity in the X-band frequency range (9.4 GHz). For the measurements within the temperature range from 6 up to 296 K, the ER 4112HV variable temperature helium-flow cryostat was applied. The EPR experiments were carried out using the following parameters: microwave power – 1.5 mW, modulation frequency – 100 kHz, modulation amplitude – 0.1...0.4 mT (depending on the EPR linewidth), conversion time – 60...120 ms (depending on the signal-to-noise ratio), and spectral resolution – 1024 points. We have used 1.1-diphenyl-2-picrylhydrazyl (DPPH) ($g = 2.0036$) as a standard sample. The investigated samples were placed into the tube with an outside diameter of 4 mm made from synthetic silica to eliminate E' center defects and other paramagnetic contaminations. The EPR spectra were simulated using the EasySpin 5.2.28 software package [10].

3. Experimental results

No EPR spectra were detected in the initial fumed silica. The EPR spectra were detected in $SiO_2:C:Zn$ samples obtained with $Zn(acac)_2$ solution of various concentrations shown in Fig. 1. However, in $SiO_2:C:Zn$ samples obtained with 1% $Zn(acac)_2$ the EPR spectra were not detected before thermal annealing due to the low spin concentration of paramagnetic centers ($N_S < 10^9$ spins/mm³). After thermal annealing at $600\text{ }^\circ\text{C}$, these samples revealed a weak EPR signal with an overall spin concentration of about $N_S \sim 5.4 \cdot 10^9$ spins/mm³ at $T = 296\text{ K}$.

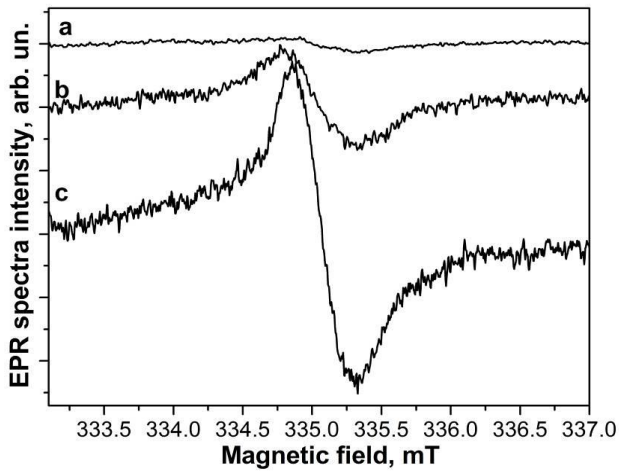


Fig. 1. The EPR spectra measured in $\text{SiO}_2\text{:C:Zn}$ samples at $T = 296$ K obtained with 1% $\text{Zn}(\text{acac})_2$ after thermal annealing at 600°C (a) and 4% $\text{Zn}(\text{acac})_2$ before (b) and after thermal annealing at 600°C (c).

As can be seen from Fig. 1, in the $\text{SiO}_2\text{:C:Zn}$ samples obtained with 4% $\text{Zn}(\text{acac})_2$, the EPR spectra were recorded both before and after thermal annealing with an overall spin concentration estimated as $N_S \sim 3.1 \cdot 10^{11}$ spins/ mm^3 before annealing and $N_S \sim 6.7 \cdot 10^{11}$ spins/ mm^3 after thermal treatment at $T = 296$ K. Since the maximum spin concentration of paramagnetic centers was found in $\text{SiO}_2\text{:C:Zn}$ samples obtained with 4% $\text{Zn}(\text{acac})_2$, the detailed analysis of EPR spectra will be further focused on these samples.

The temperature behavior of EPR spectra measured in $\text{SiO}_2\text{:C:Zn}$ samples obtained with 4% $\text{Zn}(\text{acac})_2$ annealed at 600°C shown in Fig. 2 indicates that the EPR spectra intensity increases with the temperature decrease. The simulation of the EPR spectra measured at different temperatures allowed us to distinguish three overlapping signals in the EPR spectrum of annealed $\text{SiO}_2\text{:C:Zn}$ samples obtained with 4% $\text{Zn}(\text{acac})_2$ as shown in Fig. 3. Three EPR lines have Lorentzian lineshape and are related to the paramagnetic centers with $S = 1/2$. The first EPR signal labeled as I1 has $g = 2.0029(3)$, the second EPR signal labeled as I2 has $g = 2.0042(3)$, and the third EPR signal with the lowest intensity labeled as I3 has $g = 2.0062(3)$. The I1 and I2 EPR signals have temperature-dependent linewidth and intensity in the temperature interval from 296 down to 10 K, whereas the I3 EPR signal has temperature-independent parameters.

The EPR signal I1 with $g = 2.0029(3)$ was attributed to the carbon dangling bonds (CDB), which are known to have the g -values within the range of 2.0022...2.0035 [11]. The g -value of the I2 EPR signal ($g = 2.0042(3)$) fits well with the g -values of the carbon-related radicals (CRR), which may vary between 2.0030 and 2.0042 depending on the presence of oxygen in the nearest environment of CRD [12]. Therefore, I2 EPR signal with $g = 2.0042(3)$ was assigned to the oxygen-centered CRR (single electron “centered” on the oxygen:

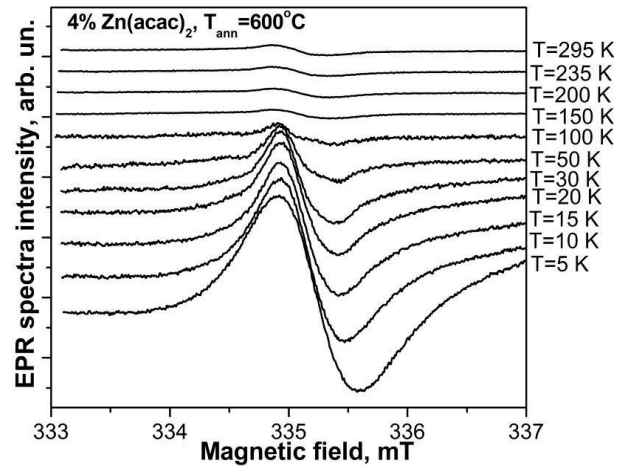


Fig. 2. The temperature dependence of EPR spectra measured in the annealed $\text{SiO}_2\text{:C:Zn}$ samples obtained with 4% $\text{Zn}(\text{acac})_2$.

$\text{RO}\cdot$ or $\text{ROO}\cdot$, where R – hydrocarbon radical), which was previously observed in $\text{SiO}_2\text{:C}$ nanocomposites [13, 14].

Following the conclusion made in [15–17], the EPR signals from CRR with sp^2 - and sp^3 -hybridization exhibit different EPR linewidth. For sp^2 -hybridized carbon atoms, the EPR linewidth should be broader than 1 mT, while for sp^3 -hybridized carbon bonds, the EPR linewidth is usually narrower than 1 mT. Therefore, since the CDB and oxygen-centered CRR centers have the EPR linewidth narrower than 1 mT, we have attributed them to the centers in a sp^3 -hybridized carbon state.

The weak I3 EPR signal with $g = 2.0062(3)$ and the linewidth close to 0.5 mT was attributed to the threefold-coordinated silicon (Si) dangling bonds that can be formed due to the oxygen presence and formation of oxidized Si on the surface of the nanocomposites [18–20]. We should note that no EPR signals corresponding to paramagnetic centers generally observed in ZnO were detected.

Fig. 4 represents the temperature dependence of the integrated intensity of CDB and oxygen-centered CRR signals was obtained by simulation of the EPR spectra, which can be described theoretically by the following equation:

$$I(T) = C/(T - \theta), \quad (1)$$

where C is the temperature-independent constant, θ is the Curie–Weiss constant (in K) related to the interaction between paramagnetic centers (generally exchange interaction).

From the fitting of Eq. (1) to the experimental data shown in Fig. 4, we have obtained the following values of Curie–Weiss constant for CDB and oxygen-centered CRR: $\theta = 0.5$ K and $\theta = 2.4$ K, respectively. The positive and small value of the Curie–Weiss constant hints at the weak ferromagnetic interaction that occurred in the system of CDB and oxygen-centered CRR.

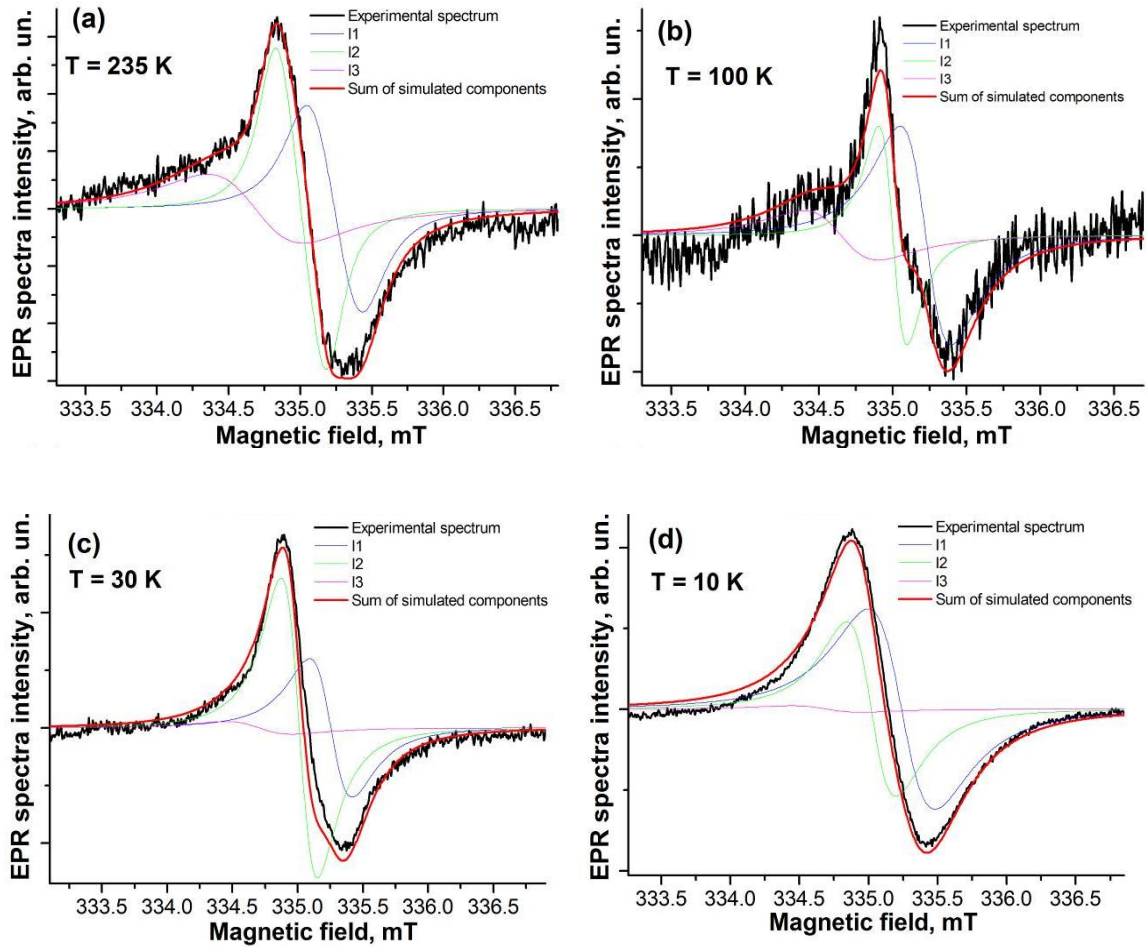


Fig. 3. Experimental (black lines), simulated components of EPR spectra (blue, green and magenta lines) and the sum of simulated components (red lines) of EPR signals in the annealed $\text{SiO}_2\text{:C:Zn}$ samples obtained with 4% $\text{Zn}(\text{acac})_2$. (a) – $T = 235$ K, (b) – 100 K, (c) – 30 K, (d) – 10 K. (Color online.)

Fig. 5 shows the temperature dependence inherent to the EPR linewidth for CDB and oxygen-centered CRR obtained from the EPR spectra simulation. The observed increase of the EPR linewidth for CDB and oxygen-centered CRR with the temperature decrease can be explained by the influence of exchange interaction between the spins in the system of carbon-related paramagnetic centers [21–23].

Considering the low spin concentration of the observed paramagnetic centers, the distance between them in the case of homogeneous distribution should be too large ($R = 0.55 \cdot N_s^{-1/3}$ [24]), and the exchange interaction can be questioned in our system. However, in the case of clusterization of paramagnetic centers, the exchange interactions between paramagnetic species become increasingly effective [25]. Therefore, we may suggest that the carbon-related centers are clustered in $\text{SiO}_2\text{:C:Zn}$ nanocomposites confirming the assumption about the sub-nanometer Zn:O:C clusters/agglomerates in aged $\text{Zn}(\text{acac})_2/\text{C}_2\text{H}_5\text{OH}$ [8, 9].

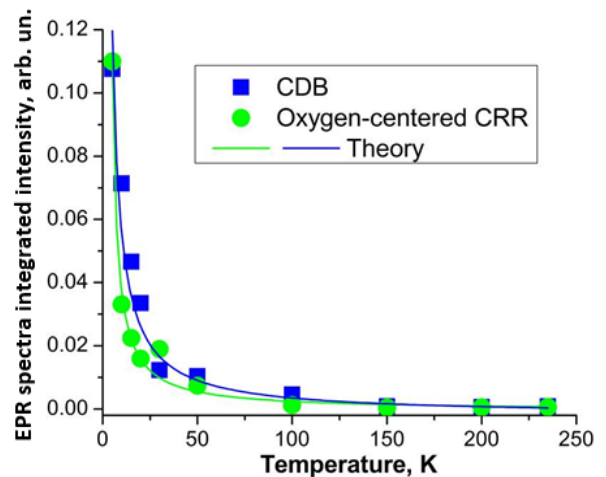


Fig. 4. Temperature dependence of the EPR signal integrated intensity for CDB and oxygen-centered CRR obtained from the simulation of EPR spectra in the annealed $\text{SiO}_2\text{:C:Zn}$ samples obtained with 4% $\text{Zn}(\text{acac})_2$. Dots – experimental data, lines – fitting with Eq. (1).

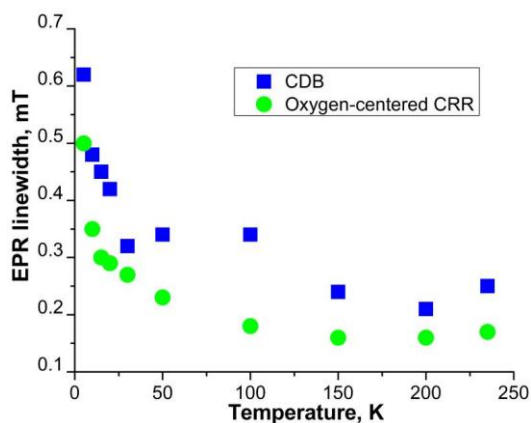


Fig. 5. The temperature dependence of EPR linewidth for CDB and oxygen-centered CRR obtained from the simulation of EPR spectra in the annealed $\text{SiO}_2\text{:C:Zn}$ samples obtained with 4% $\text{Zn}(\text{acac})_2$.

Taking into account that the carbon dangling bonds act as nonradiative recombination centers in carbon-containing materials [26], we may suggest that the presence of the oxygen-centered CRR in the sp^3 -hybridized state is responsible for the previously observed PL in the aged $\text{Zn}(\text{acac})_2/\text{C}_2\text{H}_5\text{OH}$ solution.

4. Conclusions

Using the EPR technique, we have studied the $\text{SiO}_2\text{:C:Zn}$ nanocomposites prepared using infiltration of fumed silica with luminescent aged $\text{Zn}(\text{acac})_2$ ethanol solution of various concentrations before and after thermal annealing at 600 °C. We have found that the increase in the concentration of $\text{Zn}(\text{acac})_2$ solution and thermal annealing give rise to the increase in the spin concentration of the paramagnetic centers in $\text{SiO}_2\text{:C:Zn}$ nanocomposites. Using EPR spectra simulation, we have distinguished three overlapping EPR lines in the $\text{SiO}_2\text{:C/Zn}$ nanocomposites, which were attributed to the carbon dangling bonds, silicon dangling bonds and oxygen-centered carbon radicals. Weak ferromagnetic exchange interaction in the system of carbon-related centers was found. It was supposed that the carbon-related centers are clustered in $\text{SiO}_2\text{:C:Zn}$ nanocomposites. The analysis of obtained results allows us to conclude that the oxygen-centered carbon radicals in the sp^3 -hybridized state should be related to light emission centers in the $\text{Zn}(\text{acac})_2/\text{C}_2\text{H}_5\text{OH}$ solution.

Acknowledgment

This work was supported by the Ministry of Education and Sciences of Ukraine (Project F2211). D.V. Savchenko acknowledges Operational Program Research, Development and Education financed by European Structural and Investment Funds and the Czech Ministry of Education, Youth and Sports, Project SOLID21 CZ.02.1.01/0.0/0.0/16_019/0000760. The authors also thank anonymous referees for their constructive comments that improved the manuscript.

References

- Oranska O.I., Danylenko M.I., Bogatyrev V.M., Gornikov Y.I. Structure of modifying component in nanocomposites based on fumed silica and Mg, Mn, Ni, Zn oxides. *Khimiya, Fizyka ta Tekhnologiya Poverhni*. 2011. **2**, No 3. P. 258–261 (in Russian). <https://www.cpts.com.ua/index.php/cpts/article/view/98>.
- Bogatyrev V.M., Borysenko L.I., Oranska O.I., Galaburda M.V. $\text{M}_x\text{O}_y/\text{SiO}_2$ nanocomposites based on fumed silica and acetates of Ni, Mn, Cu, Zn, Mg. *Poverhnya*. 2009. **15**. P. 294–302 (in Russian). <https://surfacezbir.com.ua/index.php/surface/article/view/351>.
- Bogatyrev V.M., Oranska O.I., Gun'ko V.M. *et al.* Influence of metal content on structural characteristics of inorganic nanocomposites $\text{M}_x\text{O}_y/\text{SiO}_2$ and $\text{C/M}_x\text{O}_y/\text{SiO}_2$. *Khimiya, Fizyka ta Tekhnologiya Poverhni*. 2011. **2**, No 2. P. 135–146 (in Russian). <https://www.cpts.com.ua/index.php/cpts/article/view/83>.
- Gun'ko V.M., Turov V.V., Leboda R. Structure-adsorption characteristics of carbon–oxide materials. *Theor. Exp. Chem*. 2002. **38**, No 4. P. 199–228. <https://doi.org/10.1023/A:1020586713911>.
- Gun'ko V.M., Skubiszewska-Zięba J., Leboda R. *et al.* Pyrocarbons prepared by carbonisation of polymers adsorbed or synthesised on a surface of silica and mixed oxides. *Appl. Surf. Sci.* 2004. **227**, Nos 1–4. P. 219–243. <https://doi.org/10.1016/j.apsusc.2003.11.077>.
- Leboda R., Skubiszewska-Zięba J., Rynkowski J. Preparation and porous structure of carbon-silica adsorbents obtained on the basis of Ti, Co, Ni, Cr, Zn and Zr acetylacetonates and acetylacetone. *Colloids & Surfaces A*. 2000. **174**, No 3. P. 319–328. [https://doi.org/10.1016/S0927-7757\(00\)00585-9](https://doi.org/10.1016/S0927-7757(00)00585-9).
- Turov V.V. and Leboda R. Changes in hydration properties of silica gel in a process of its carbonization by pyrolysis of acetylacetone Zn (Ti) acetylacetonates. *J. Colloid Interface Sci.* 1998. **206**, No 1. P. 58–65. <https://doi.org/10.1006/jcis.1998.5659>.
- Vasin A., Kysil D., Rudko G., Isaieva O. Visible photoluminescence of aged $\text{Zn}(\text{acac})_2/\text{C}_2\text{H}_5\text{OH}$ solution: emission/excitation/kinetics study. *Proc. Intern. Research and Practice Conference "Nanotechnology and Nanomaterials" (NANO-2017)*, 23-26 August 2017, Chernivtsi, Ukraine, p. 338. <http://ekmair.ukma.edu.ua/handle/123456789/13067>
- Vasin A.V., Kysil D.V., Isaieva O.F. *et al.* Evolution of UV/VIS photoluminescence of aged $\text{Zn}(\text{acac})_2$ solutions in correlation with carbon precipitation. *ECS Trans.* 2021. **102**, No. 1. P. 55–64. <https://doi.org/10.1149/10201.0055ecst>.
- Stoll S. and Schweiger A. EasySpin, a comprehensive software package for spectral simulation and analysis in EPR. *J. Magn. Reson.* 2006. **178**, No 1. P. 42–55. <https://doi.org/10.1016/j.jmr.2005.08.013>.

11. Barklie R.C. Characterization of defects in amorphous carbon by electron paramagnetic resonance. *Diam. Relat. Mater.* 2003. **12**, No 8. P. 1427–1434. [https://doi.org/10.1016/S0925-9635\(00\)00465-9](https://doi.org/10.1016/S0925-9635(00)00465-9).
12. Haenen K., Meykens K., Nesládek M. *et al.* Phonon-assisted electronic transitions in phosphorus-doped n-type chemical vapor deposition diamond films. *Diam. Relat. Mater.* 2001. **10**, Nos 3-7. P. 439–443. [https://doi.org/10.1016/S0925-9635\(00\)00511-2](https://doi.org/10.1016/S0925-9635(00)00511-2).
13. Savchenko D.V., Vorlíček V., Kalabukhova E.N. *et al.* Infrared, Raman and magnetic resonance spectroscopic study of SiO₂:C nanopowders. *Nanoscale Res. Lett.* 2017. **12**. P. 292-1–292-12. <https://doi.org/10.1186/s11671-017-2057-1>.
14. Savchenko D., Kalabukhova E., Sitnikov A. *et al.* Magnetic resonance and optical study of carbonized silica obtained by pyrolysis of surface compounds. *Adv. Mat. Res.* 2014. **854**. P. 99–104. <https://doi.org/10.4028/www.scientific.net/AMR.854.99>.
15. Trassl S., Motz G., Rössler E., Ziegler G. Characterization of the free-carbon phase in precursor-derived Si-C-N ceramics: I, Spectroscopic methods. *J. Am. Ceram. Soc.* 2004. **85**, No 1. P. 239–244. <https://doi.org/10.1111/j.1151-2916.2002.tb00072.x>.
16. Prasad B.L.V., Sato H., Enoki T. *et al.* Heat-treatment effect on the nanosized graphite π -electron system during diamond to graphite conversion. *Phys. Rev. B.* 2000. **62**, No 16. P. 11209–11218. <https://doi.org/10.1103/PhysRevB.62.11209>.
17. Erdem E., Mass V., Gembus A. *et al.* Defect structure in lithium-doped polymer-derived SiCN ceramics characterized by Raman and electron paramagnetic resonance spectroscopy. *Phys. Chem. Chem. Phys.* 2009. **11**, No 27. P. 5628–5633. <https://doi.org/10.1039/b822457a>.
18. Cantin J., Schoisswohl M., von Bardeleben H. *et al.* P_{b1} defect study and chemical characterization of the Si(001) SiO₂ interface in oxidized porous silicon. *Surf. Sci.* 1996. **352-354**. P. 793–796. [https://doi.org/10.1016/0039-6028\(95\)01230-3](https://doi.org/10.1016/0039-6028(95)01230-3).
19. Mrozowski S. Specific heat anomalies and spin-spin interactions in carbons: A review. *J. Low Temp. Phys.* 1979. **35**, Nos 3-4. P. 231–298. <https://doi.org/10.1007/BF00115580>.
20. Izumi T., Show Y., Deguchi M. *et al.* Electron spin resonance study of diamond-like nuclei produced in an Si surface layer by high dose C ion doping. *Thin Solid Films.* 1993. **228**, Nos 1-2. P. 285–288. [https://doi.org/10.1016/0040-6090\(93\)90617-X](https://doi.org/10.1016/0040-6090(93)90617-X).
21. Misra S.K. Role of exchange interaction in effecting spin-lattice relaxation: Interpretations of data on Cr³⁺ in Cu_{2+x}Cr_{2x}Sn_{2-2x} spinel and dangling bonds in amorphous silicon. *Phys. Rev. B.* 1998. **58**, No 22. P. 14971–14977. <https://doi.org/10.1103/PhysRevB.58.14971>.
22. Andronenko S.I., Stiharu I., Misra S.K. Synthesis and characterization of polyureasilazane derived SiCN ceramics. *J. Appl. Phys.* 2006. **99**, No 11. P. 113907-1–113907-5. <https://doi.org/10.1063/1.2202291>.
23. Savchenko D., Kulikovskiy V., Vorlíček V. *et al.* Optical and magnetic resonance study of a-SiC_xN_y films obtained by magnetron sputtering. *phys. status solidi (b)*. 2014. **251**, No 6. P. 1178–1185. <https://doi.org/10.1002/pssb.201451041>.
24. Hoch M.J.R., Reynhardt E.C. Nuclear spin-lattice relaxation of dilute spins in semiconducting diamond. *Phys. Rev. B.* 1998. **37**, No 16. P. 9222–9226. <https://doi.org/10.1103/PhysRevB.37.9222>.
25. Shames A.I., Panich A.M., Mogilko E. *et al.* Magnetic resonance study of fullerene-like glassy carbon. *Diam. Relat. Mater.* 2007. **16**, No 12. P. 2039–2043. <https://doi.org/10.1016/j.diamond.2007.08.020>.
26. Vasin A.V., Rusavsky A.V., Lysenko V.S. *et al.* The influence of vacuum annealing temperature on the fundamental absorption edge and structural relaxation of a-SiC:H films. *Semiconductors.* 2005. **39**, No 5. P. 572–576. <https://doi.org/10.1134/1.1923567>.

Authors and CV



Dariya V. Savchenko, Doctor of Sciences in Physics and Mathematics, Associate Professor at the Department of General Physics and Solid State Physics of the National Technical University of Ukraine “Igor Sikorsky Kyiv Polytechnic Institute” and Scientist at the Department of Analysis of Functional Materials, Institute of Physics, Czech Academy of Sciences. The area of her scientific interests includes magnetic resonance studying the semiconductors, dielectrics and biomaterials. ORCID: 0000-0002-0005-0732.



E-mail: memonvs@gmail.com.

Valentyn S. Memon, Master student at the Department of General Physics and Solid State Physics of the National Technical University of Ukraine “Igor Sikorsky Kyiv Polytechnic Institute”. The area of his scientific interests includes magnetic resonance in nanocomposites.



Oleksandr P. Kuz, Lecturer at the Department of General Physics and Solid State Physics of the National Technical University of Ukraine “Igor Sikorsky Kyiv Polytechnic Institute”. The area of his scientific interests includes magnetic properties of nanostructures. ORCID: 0000-0002-0994-5647.

E-mail: a.kuz@kpi.ua



Andrii V. Vasin, Doctor of Sciences in Physics and Mathematics, Researcher at the Department of General Physics and Solid State Physics of the National Technical University of Ukraine “Igor Sikorsky Kyiv Polytechnic Institute” and Leading Research Fellow at the

Department of Functional Materials and Structures, V. Lashkaryov Institute of Semiconductor Physics, NAS of Ukraine. The area of his scientific interests includes the materials science and technology of functional materials, primarily carbon related nanocomposites and thin films.

ORCID: 0000-0003-2771-0670.

E-mail: av966@yahoo.com

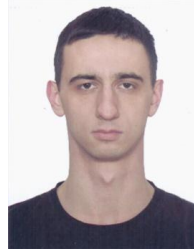


Andrii V. Rusavsky, PhD in Physics and Mathematics, Researcher at the Department of General Physics and Solid State Physics of the National Technical University of Ukraine “Igor Sikorsky Kyiv Polytechnic Institute” and Senior Research Fellow at the Department

of Functional Materials and Structures, V. Lashkaryov Institute of Semiconductor Physics, NAS of Ukraine. The area of his scientific interests includes materials science and technology of functional materials, primarily carbon related nanocomposites and thin films.

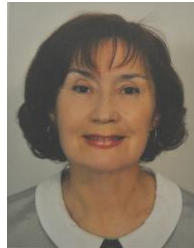
ORCID: 0000-0001-6386-3434.

E-mail: rusavsky@yahoo.com



Dmytro V. Kysil, PhD, Research Fellow at the Department of Functional Materials and Structures, V. Lashkaryov Institute of Semiconductor Physics, NAS of Ukraine. The area of his scientific interests includes fabrication and properties of carbon-containing functional composites. ORCID: 0000-0003-4637-9397.

E-mail: kdmitr93@gmail.com



Faina M. Gareeva, Doctor of Sciences in Physics and Mathematics, Associate Professor at the Department of General Physics and Solid State Physics of the National Technical University of Ukraine “Igor Sikorsky Kyiv Polytechnic Institute”. The area of her scientific interests includes magnetism in nanostructured

materials. ORCID: 0000-0003-4714-3060.

E-mail: fainamax51@gmail.com



Ekaterina N. Kalabukhova, Doctor of Sciences in Physics and Mathematics, Leading Researcher at the Department of Semiconductor Heterostructures, V. Lashkaryov Institute of Semiconductor Physics, NAS of Ukraine. The area of her scientific interests

includes magnetic resonance in semiconductor and nanosized materials. ORCID: 0000-0003-0272-9471.

E-mail: kalabukhova@yahoo.com

Дослідження методом ЕПР парамагнітних центрів у нанокompозитах $\text{SiO}_2\text{:C:Zn}$, отриманих інфільтрацією люмінесцентним розчином $\text{Zn}(\text{acac})_2$

Д.В. Савченко, В.С. Мемон, А.В. Васін, Д.В. Кисіль, А.В. Русавський, О.П. Кузь, Ф.М. Гарєєва, К.М. Калабухова

Анотація. Кремнезем-вуглецеві нанокompозити з цинком ($\text{SiO}_2\text{:C:Zn}$), отримані шляхом інфільтрації витриманим етаноловим розчином ацетилацетонату цинку ($\text{Zn}(\text{acac})_2$) різної концентрації (1% та 4%) до матриці пірогенного кремнезему (SiO_2), вивчались методом ЕПР у температурному інтервалі від 6 до 296 К до та після термічного відпалу. Спектр ЕПР $\text{SiO}_2\text{:C:Zn}$ нанокompозитів складається з трьох смуг Лоренцевої форми, пов'язаних із парамагнітними центрами з $S = 1/2$, які було віднесено до обірваних зв'язків вуглецю (CDB) ($g = 2.0029(3)$), обірваних зв'язків кремнію ($g = 2.0062(3)$) та киснево-центрованих вуглецевмісних радикалів (CRR) ($g = 2.0042(3)$). Мала ширина лінії ЕПР (<1 мТ), що спостерігалась для CDB та киснево-центрованих CRR, дозволила віднести ці центри до sp^3 -гібридизованого стану. Виявлено, що температурна залежність інтегральної інтенсивності сигналів ЕПР від CDB та киснево-центрованих CRR описується законом Кюрі–Вейса з додатним значенням константи Кюрі–Вейса малої величини, що вказує на те, що у спіновій системі CDB та киснево-центрованих CRR існує слабка феромагнітна обмінна взаємодія. Висунуто припущення, що у $\text{SiO}_2\text{:C:Zn}$ нанокompозитах здійснюється кластеризація вуглецевмісних центрів. Зроблено висновок, що киснево-центровані CRR у sp^3 -гібридизованому стані відповідають за попередньо спостережену інтенсивну фотолюмінесценцію розчину $\text{Zn}(\text{acac})_2/\text{C}_2\text{H}_5\text{OH}$.

Ключові слова: кремнезем-вуглецеві нанокompозити, вуглецевмісні центри, обірвані зв'язки, обмінна взаємодія, електронний парамагнітний резонанс.